# EFFECTS OF METHANE ADDITION ON THE LAMINAR BURNING VELOCITY AND MARKSTEIN LENGTH OF METHANOL/AIR PREMIXED FLAME

***Haiqing SHEN[a], Huihong LIAO[b], Qiyang WANG[c], Cangsu XU[c], Kai LIU[c], Wenhua ZHOU[c*]***

[a]Taizhou Vocational College of Science & Technology, Taizhou, China P.R.

[b]Vehicle Engineering Center-CAE Technology Development, Geely Automobile Research Institute, Ningbo, China P.R.

[c]College of Energy Engineering, Zhejiang University, Hangzhou, China P.R.

*Corresponding author; E-mail: zwh114@zju.edu.cn

*Adding methane to methanol can solve the problem of difficult cold starts of methanol engines. Therefore, it is important to understand the combustion of methane and methanol fuel blends. Because of this, this study explores the effect of methane addition on the laminar burning velocity and Markstein length of methanol/methane premixed flames under stoichiometric conditions at the initial temperatures of 353 K, 373 K, and 393 K, initial pressures of 1 bar, 2 bar, and 4 bar, using methane addition ratios of 0%, 25%, 50%, 75% and 100% in a constant volume combustion chamber. The results show that the laminar burning velocity decreases linearly with the increase of methane addition ratio due to the linear decrease of the Arrhenius factor. The sensitivity analysis revealed that the kinetic effect is the main reason for the inhibition of laminar burning velocity, which is insensitive to initial temperature but enhanced at a high initial pressure. The Markstein length decreases with the addition of methane and the increase of initial pressure, which is mainly caused by the high mass diffusivity of methane and the decrease of flame thickness due to the increase of initial pressure.*

Key words*: Methanol, Methane, Laminar burning velocity, Markstein length*

## 1. Introduction

Methanol as an alternative fuel to diesel and gasoline in ICEs has attracted extensive attention [1]. Moreover, in recent years, renewable methanol has helped methanol engines achieve almost zero $CO_2$ emissions, showing greater advantages than other fuels. In general, methanol has unique properties [2]. Its high oxygen content means that it requires less air for complete combustion than gasoline or diesel. It has no C-C bond, so it is not easy to form long-chain hydrocarbons and particles during combustion. It has good knock resistance and fast laminar burning velocity and can be used in ICEs with a higher compression ratio without knocking, which is beneficial for thermal efficiency and reducing engine size. It has a low adiabatic flame temperature, which means less wall heat loss and NOx. Its high gasification latent heat also reduces in-cylinder and intake port temperature and increases the intake density. However, due to its high low flammability limit (LFL) and low vapor

pressure, cold starting the engine becomes difficult, which is a drawback for methanol engines [3]. Methane/methanol dual fuel engines are of particular concern because they are regarded as green fuels and can reduce $CO_2$ emissions compared to traditional fuels. More importantly, on the one hand, the addition of methane can eliminate the difficulty of cold starting methanol engines [4]. On the other hand, the enrichment of methanol can improve the complete combustion of methane, leading to higher thermal efficiency and lower HC and CO emissions [5].

Laminar burning velocity (LBV) embodies the diffusivity, heat release, and chemical reaction rate of combustible mixtures, which is of great significance for verifying chemical reaction mechanisms and guiding engine design optimization [6]. The LBV of binary fuel blends containing methane or methanol has been extensively studied [7-9] but focused on adding methane or methanol as an additive to gasoline and diesel [10-12]. Recently, Wang et al. [13] measured the laminar combustion characteristics of methanol/methane mixtures under different working conditions and performed chemical kinetic analysis. Although Wang et al. [13] measured the partially laminar combustion characteristics of methanol/methane mixtures, they used the constant volume method to calculate the LBV. Compared with the constant pressure method, this method has larger errors due to the use of more assumptions [14]. More importantly, this method cannot measure the Markstein length, which reflects the stability of the flame, and the high diffusivity of methane will significantly affect the stability of the flame, which is very important in the application of ICEs. At the same time, Wang et al. [13] only uses one mechanism for simulations, leading to very limited results. In addition, although kinetic effects have been shown to play an important role, the high diffusivity of methane and the resulting change in the adiabatic flame temperature of the mixed fuel also have a potential impact on LBV, which requires further analysis.

To sum up, methane addition is one of the best pathways to solve the problem of difficult cold starting of methanol engines due to its high LFL and low vapor pressure. However, the influence of methane on methanol LBV is still insufficiently studied, which is crucial to optimize the performance of methane/methanol engines and is worthy of in-depth study. In this study, the LBV and Markstein length of methane/methanol under different working conditions are measured by the constant pressure method, the LBVs calculated by various mechanisms are compared, the factors affecting the Markstein length are discussed, and the influence of fuel mixing on thermal effect, diffusion effect and kinetic effect is analyzed using one-step overall reaction assumption. This study provides theoretical knowledge for the application of methane in methanol engines.

## 2. Experimental and computational specifications

### 2.1. Experimental setup

Detailed experimental devices and steps can be found in Ref. [15] and Ref. [13]. The main devices are briefly described below. As shown in Figure 1, combustion chamber is a cube with a volume of 2.067 L, which can be heated by heating resistors installed inside it. A pair of quartz glasses with a diameter of 105 mm are installed on its side for schlieren imaging. The temperature sensor and precision pressure gauge are used to measure the initial temperature and initial pressure. Liquid fuel is injected into combustion chamber through micro syringe, and combustible gas and air are inflated through precision pressure reducing valve and mass flow controller. The ignition signal is sent out by the ignition control module and the high-speed camera is triggered by the digital delay generator to

shoot the flame image. The recording speed is 12800 fps and the resolution of flame images is 1024 × 1024 pixels.

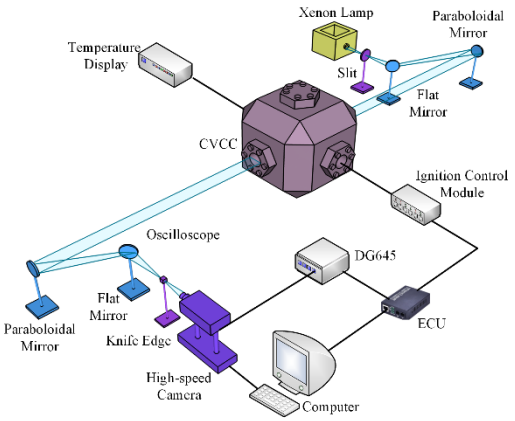


**Fig. 1. Experimental setup**

Methane and methanol are mixed by mole fraction, so the methane addition ratio $X_{Me}$ can be expressed by $X_{Me} = n_{CH4}/(n_{CH4} + n_{CH3OH})$, where $n_{CH3OH}$ and $n_{CH4}$ are the moles of methanol and methane, respectively.Since methane enters combustion chamber by mixing with air in advance, the mixing ratio of methane/air $k_{Me/A}$ can be calculated as $k_{Me/A} = 0.21X_{Me}/[2 - 0.5(1 - X_{Me})]$.

### 2.2. Data processing

The method of calculating LBV used in current work has been widely used [16]. According to the flame radius ($r_f$) in the flame image at different times ($t$), the stretching flame speed ($S_b$) can be calculated as $S_b = dr_f/dt$. Then, calculate the stretch rate ($K$) of the spherical flame by $K = 2\,S_b/r_f$, and the unstretched flame speed is obtained by extrapolation according to Eq. (1) [17].

$$\left(\frac{S_b}{S_b^0}\right)^2 ln\left(\frac{S_b}{S_b^0}\right)^2 = -2\frac{L_b K}{S_b^0} \tag{1}$$

where $L_b$ is the Markstein length. Figure 2 shows the extrapolation process, it should be noted that according to the assumption of quasi-steady flame, a radius of 8-20 mm is selected for the extrapolation to reduce the influence of ignition, pressure rise, and wall confinement of the combustion chamber [18].

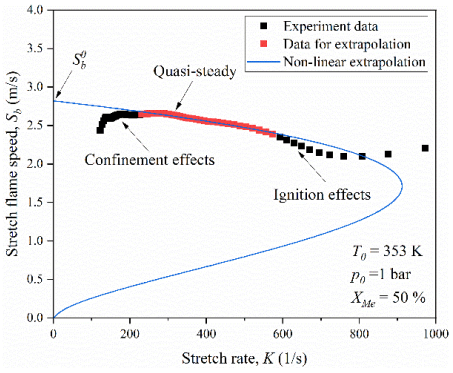


**Fig. 2. Extrapolation model for methanol/methane/air mixtures at the initial temperature $T_0 = 353$ K, initial pressure $p_0 = 1$ bar and methane addition ratio $X_{Me} = 50\%$**

The laminar burning velocity $S_L^0$ can be calculated by $S_L^0 = S_b^0 \rho_b / \rho_u$, where $\rho_b$ and $\rho_u$ are the densities of the burned and unburned gases, respectively, calculated using CANTERA. CANTERA was also used to calculate the numerical LBV of methanol/methane/air mixtures. The multicomponent transport model was adopted and thermal diffusion was considered. The ratio, slope, and curve settings were 3, 0.06, and 0.12, respectively. The well-validated methanol mechanisms, including Li [19], San Diego [20], Zhang et al. [21], and Aramco 1.3 [22] were used.

### 2.3. Experimental uncertainties

In order to verify the experimental results and consider the experimental uncertainty, in a pre-experiment for this study, the LBV of methanol was measured as shown in Figure 3, and compared with experimental data in the literature [23-26] and simulation results for different methanol mechanisms. The simulation results are greater than the experimental results, especially in the rich mixture. Under the stoichiometric ratio, the deviation between the results of this experiment and the average results of each experiment in literature is 6.17%. Among the results of each model, the deviation from the Zhang model [21] is the smallest at 12.69%. Therefore, the error of this experiment is within an acceptable range, but the model still needs further optimization. At the same time, each experiment was repeated three times, so that the confidence interval of the data was within 95%.

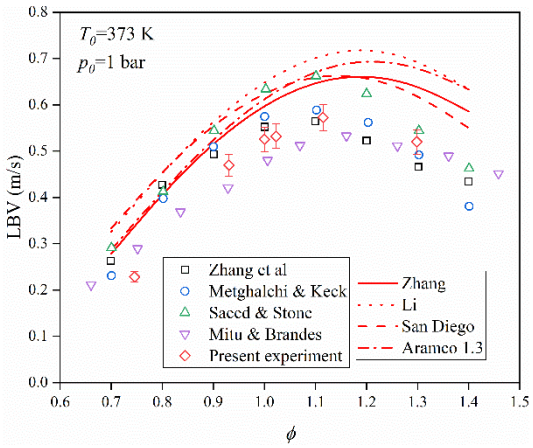


**Fig. 3. Comparison of LBV of methanol at $p_0$ = 1 bar and $T_0$ = 373 K. Mitu and Brandes [23], Zhang et al [24], Saeed and Stone [25] , Metghalchi and Keck [26]**

## 3. Result and discussion

### 3.1. Laminar burning velocity

Figure 4 shows the change in LBV with $X_{Me}$ under different working conditions. This study's data are compared to the experimental results of Wang et al [13] and the simulation results of different mechanisms. There are some differences in the simulation results but the trend is the same, and the experimental results are smaller than the simulation results, similar to Figure 3, which is caused by the the experimental heat loss and overestimation of the key reaction in the mechanism [13]. In addition, Zhang model results are closer to the experimental results under low $X_{Me}$, while Li and San Diego models are closer to the experimental results under high $X_{Me}$. Comparing the results of Wang et al. [13] using CVM, it is found that the results of this study are generally smaller, which is similar to the results of Omari et al. [27]. The LBV decreases with increasing $p_0$, which is due to the enhancement

of important three-body chain termination reactions and increased gas density [16]. In addition, LBV increases with increasing temperature because of the increase in reaction rate caused by increasing $T_0$. Both experimental and simulated LBV decrease linearly with increasing $X_{Me}$, which is similar to Refs. [13,28].

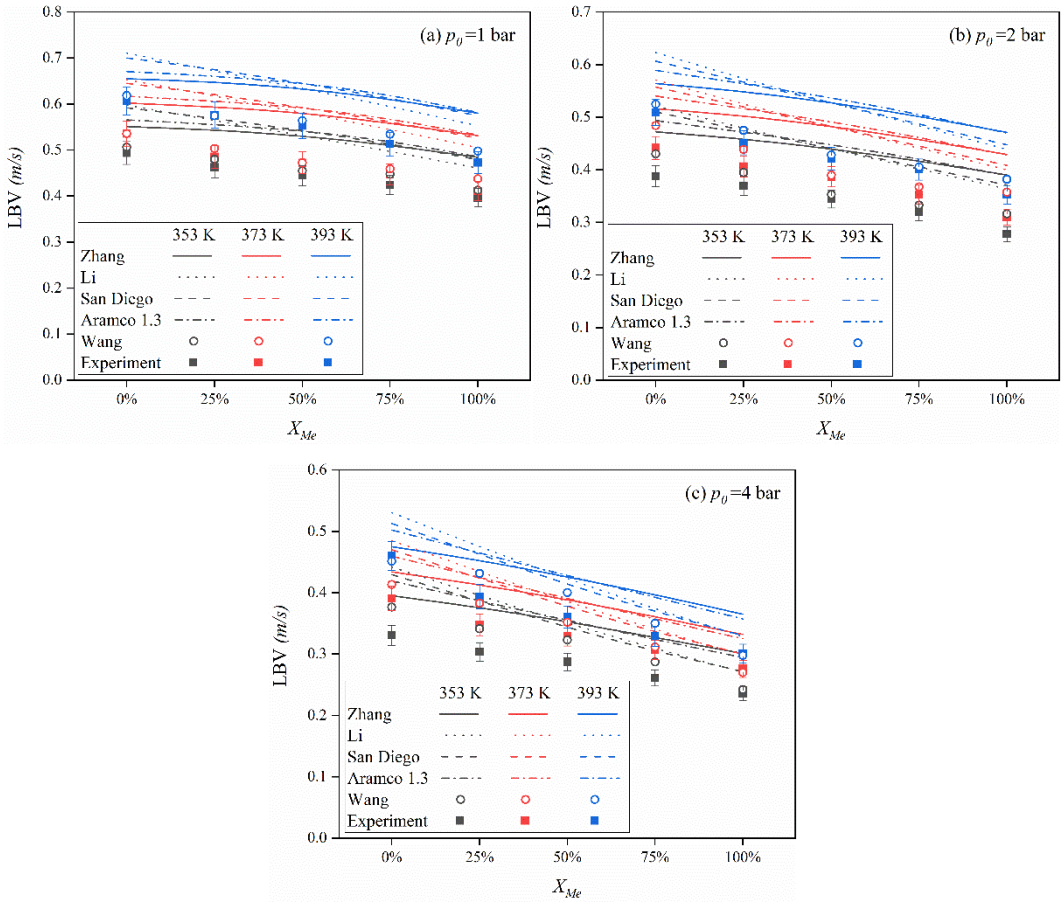


**Fig. 4. Measured and simulated LBVs of methanol/methane/air mixtures as a function of $X_{Me}$ under different $T_0$ and (a) $p_0 = 1$ bar, (b) $p_0 = 2$ bar, (c)$p_0 = 4$ bar**

In order to explore the influence of methane addition on LBV, based on the detailed expression of laminar burning flux [29] and the assumption of a one-step overall reaction, LBV can be determined by [30] Eq. (2).

$$S_L^0 \propto (\alpha Le)^{1/2} exp(-T_a/2T_{ad}) \tag{2}$$

where $T_a$ is activation temperature ($= E_a/R$), $E_a$ is the global activation energy, obtained by $-2R[\partial \ln(S_L^0 \rho_u)/\partial(1/T_{ad})]$. $R$ is a universal gas constant, and $T_{ad}$ is adiabatic flame temperature. $Le$ is the Lewis number ($= \alpha/D_m$), where $\alpha$ is thermal diffusivity, $D_m$ is mass diffusivity. In fact, the effective Lewis number of the mixed fuel is used here. The volume fraction weighting method [31] is adopted as $Le_{mix} = x_{Me} Le_{Me} + x_{MeOH} Le_{MeOH}$, where $x$ is the fuel volumetric fraction and the subscripts represent the corresponding substances. Since the equivalence ratio is 1 in this study, the effective Lewis is simplified to fuel and oxygen's average value as $(Le_O + Le_{mix})/2$ [32]. $(\alpha Le)^{1/2}$, $T_{ad}$, and $T_a$ represent diffusion, thermal, and kinetic effects, respectively [33]. Figure 5

shows the variation of $(\alpha Le)^{1/2}exp(-T_a/2T_{ad})$ with $X_{Me}$ under different working conditions. The effect of diffusion can be seen as $(\alpha Le)^{1/2}$, while the thermal and kinetic effects can be seen as a combined Arrhenius factor, represented by $exp(-T_a/2T_{ad})$ [34]. It can be found that $(\alpha Le)^{1/2}exp(-T_a/2T_{ad})$ decreases linearly with $X_{Me}$, and the change trend with $T_0$ and $p_0$ is consistent with LBV as shown in Figure 4. Therefore, Eq. (2) is verified. It should be noted that $\alpha$ caused by the addition of methane actually increases, while $Le$ decreases, $(\alpha Le)^{1/2}$ is nonlinear as shown in Figure 5, so the Arrhenius factor plays a leading role in the linear relationship.

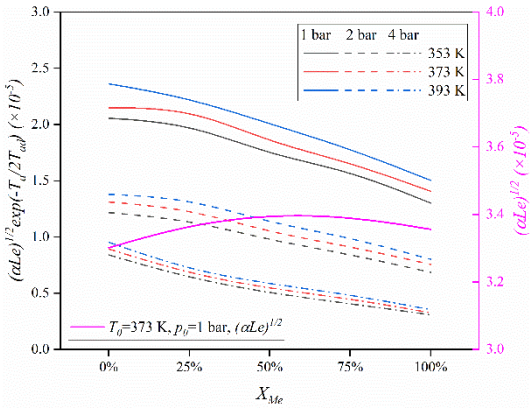


**Fig. 5. Variation of $(\alpha Le)^{1/2}exp(-T_a/2T_{ad})$ with $X_{Me}$ at $p_0$ = 1 bar, 2 bar, 4 bar and $T_0$ = 353 K, 373 K, 393 K**

In order to quantitatively determine the influence of each parameter change caused by methane addition on LBV, the kinetics, diffusion, and thermal sensitivity factors were obtained by differentiating Eqs. (3)-(6) [33,34].

$$\frac{\partial lnS_L^0}{\partial lnX_{Me}} = DF + TF + KF \tag{3}$$

$$DF = \frac{1}{2\alpha Le}\frac{d(\alpha Le)}{dlnX_{Me}} \tag{4}$$

$$TF = \frac{T_a}{2T_{ad}^2}\frac{dT_{ad}}{dlnX_{Me}} \tag{5}$$

$$KF = -\frac{1}{2T_{ad}}\frac{dT_a}{dlnX_{Me}} \tag{6}$$

where *DF*, *TF*, and *KF* are diffusion, thermal, and kinetic sensitivity factors, respectively. These parameters qualitatively represent the modifications of the diffusion, thermal, and kinetic effects due to methane addition. Figure 6 shows the variation of each influencing factor with $X_{Me}$ at different working conditions. The impact of methane addition on LBV is mainly realized through kinetic effects, which is consistent with the discussion in the literature [33,34]. *KF* is negative and decreases with $p_0$, indicating that it has an inhibitory effect on LBV and the effect is enhanced at high $p_0$, but it is not sensitive to $T_0$, mainly because $E_a$ increases with the increase of $p_0$, but changes little with $T_0$. *DF* and *TF* are very close to 0, indicating the diffusion and thermal effect is very weak, and they all change a little with $T_0$ and $p_0$. Due to the increase of $T_{ad}$ caused by the addition of methane, the

thermal effect has a weak enhancement effect on the LBV, while the reduction of $Le$ suppresses the LBV, so *TF* is positive and *DF* is negative.

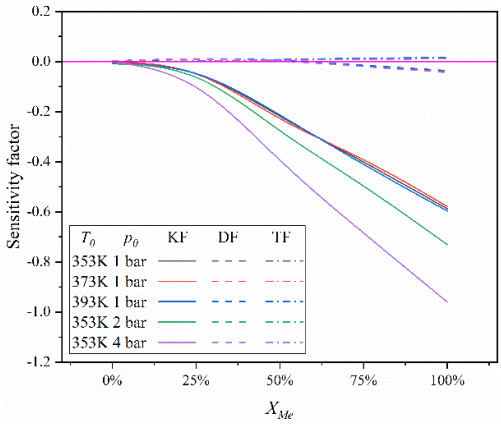


**Fig. 6. Variation of kinetics, diffusion, and thermal sensitivity factors with $X_{Me}$ at $p_0 =$ 1 bar, 2 bar, and 4 bar and $T_0 =$ 353 K, 373 K, and 393 K**

### 3.2. Markstein length

The Markstein length ($L_b$) reflects the sensitivity of flame to stretch rate. In this study, the theoretical $L_b$ is calculated using Eq. (7) [32].

$$L_b = M_b \delta_f = \left( \frac{\gamma_2 Ze(Le-1)}{2} + \frac{\gamma_1}{\sigma} \right) \delta_f \tag{7}$$

Where $\gamma_1 = 2\sigma/(\sigma^{1/2}+1)$ and $\gamma_2 = 4/(\sigma-1) \times [\sigma^{1/2} - 1 - [\ln(\sigma^{1/2}+1)]/2]$, $\sigma$ is the density ratio, obtained by $\rho_u/\rho_b$. $Ze$ is the Zeldovich number, obtained by $[T_a(T_{ad}-T_0)]/T_{ad}^2$. $\delta_f$ is the flame thickness, obtained by $(T_{ad}-T_0)/(dT/dx)_{max}$ [31]. $M_b$ is the Markstein number. Figure 7 shows the theoretical and experimental $L_b$ under various working conditions. The theoretical and experimental results have similar trends, that is, they decrease with the increase in $X_{Me}$ and $p_0$, but is less affected by $T_0$. It is noticed that under high pressure, $L_b$ decreases dramatically after adding methane, which indicates increased flame instability. It should be noted that measurement uncertainty of $L_b$ is relatively large and $L_b$ measured by different researchers can even be greater than 300% [35].

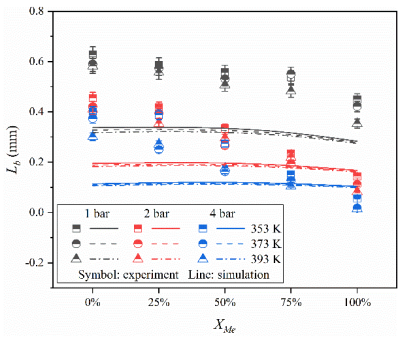


**Fig. 7. Variation of theoretical and experimental $L_b$ with $X_{Me}$ at $p_0 =$ 1 bar, 2 bar, 4 bar and $T_0 =$ 353 K, 373 K, 393 K**

According to the analysis of Law et al. [29] and Clavin et al. [36], the proportional relation between $L_b$ and its relative parameters is $L_b \sim Ze(Le-1)\sigma\delta_f$. In order to further study the influencing factors of $L_b$, Figure 8 shows the variation of each parameter including $Ma$, $Ze$, $(Le-1)$, $\sigma$, $\delta_f$ with $X_{Me}$ under different working conditions. Among them, $Ma$, $Ze$, $(Le-1)$, $\sigma$ are normalized by the reference value of the parameter ($p_0 =$ 1 bar, $T_0 =$ 353 K and $X_{Me}$ = 0%), so as to show the influence degree of the parameter. It should be noted that $Ma$ is additionally introduced into the discussion because it can control other variables and more clearly reflect the influence of $\delta_f$ on $L_b$ under different conditions. The results show that $Ma$ decreases with the addition of methane, but basically does not change with $T_0$ and $p_0$, while $\delta_f$ decreases significantly with the increase of $p_0$, indicating that the decrease of $L_b$ with $p_0$ is mainly due to the decrease of $\delta_f$. Also, $\delta_f$ plays a positive role in maintaining the stability of the methane-added flame, as it increases with $X_{Me}$. It is worth noting that, although the value of $(Le-1)$ changes slightly, it still has a greater effect on the $L_b$ compared with other parameters . Besides, $Ze$ and $\sigma$ have little effect on $L_b$, the former increases with $X_{Me}$, while the latter decreases, and they are easily affected by $p_0$ and $T_0$, respectively. Overall, the high mass diffusivity of methane and the reduced $\delta_f$ due to high $p_0$ lead to increased flame instability for methane/methanol/air mixtures.

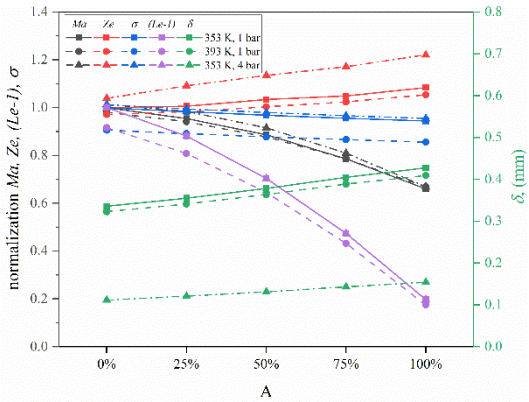


**Fig. 8. Influence of $X_{Me}$, $p_0$ and $T_0$ on the parameters related to $L_b$**

## 4. Conclusions

In this study, the effects of initial temperature, initial pressure, and methane addition ratio on the laminar burning velocity and Markstein length of a methanol/methane/air premixed flame at the stoichiometric ratio were investigated. The main results include:

The LBV of methanol/methane/air mixtures decreases linearly with the methane addition ratio and increases with increasing initial temperature and decreasing initial pressure. The simulation results are greater than the experimental results.

The reason why methane addition makes the LBV of the methanol/methane/air mixture decrease linearly is the linear decrease of the Arrhenius factor. Furthermore, the influence of the kinetic effect plays a dominant role, which is not sensitive to the initial temperature but is enhanced under high initial pressure.

The Markstein length decreases with the addition of methane and the increase of initial pressure, which is mainly caused by the high mass diffusivity of methane and the decrease of flame thickness due to the increase of initial pressure.

**Acknowledgment**

The authors are thankful to the National Natural Science Foundation of China (No. 52076010) and Ningbo Major Science and Technology Project (20212ZDYF020041) for their support.

**Nomenclature**

| | | | |
|---|---|---|---|
| $D_m$ | Mass diffusivity, [$m^2/s$] | $T_{ad}$ | Adiabatic flame temperature, [K] |
| $E_a$ | Global activation energy, [J] | $T_0$ | Initial temperature, [K] |
| $K$ | Stretch rate, [1/s] | $t$ | Flame propagation time, [s] |
| $k_{Me/a}$ | Mixing ratio of methane/air, [–] | $X_{Me}$ | Methane addition ratio, [–] |
| $L_b$ | Markstein length, [m] | $x$ | Fuel volumetric fraction, [–] |
| $Le$ | Lewis number ($=\alpha/D_m$), [–] | $Ze$ | Zeldovich number |
| $M_b$ | Markstein number ($=L_b/\delta_f$), [–] | | ($=T_a(T_{ad}-T_0)/T_{ad}^2$), [–] |
| $p_0$ | Initial pressure, [Pa] | | |
| $R$ | Universal gas constant, [$Jmol^{-1}K^{-1}$] | *Greek letters* | |
| $r_f$ | Flame radius, [m] | $\alpha$ | Thermal diffusivity, [$m^2/s$] |
| $S_b$ | Stretched flame speed, [m/s] | $\delta_f$ | Flame thickness, [m] |
| $S_b^0$ | Unstretched flame speed, [m/s] | $\rho_b$ | Densities of burned gases, [$kg/m^3$] |
| $S_L^0$ | Laminar burning velocity, [m/s] | $\rho_u$ | Densities of unburned gases, [$kg/m^3$] |
| $T_a$ | Activation temperature, [K] | $\sigma$ | Density ratio, [–] |

**Reference**

[1] Liu, C., *et al.*, Methanol as a Fuel for Internal Combustion Engines, in: Engines and Fuels for Future Transport (Eds. G. Kalghatgi, et al.), Springer Singapore, Singapore, 2022, pp. 281-324

[2] Verhelst, S., *et al.*, Methanol as a Fuel for Internal Combustion Engines, *Progress in Energy and Combustion Science, 70* (2019), pp. 43-88

[3] Gong, C., *et al*., Investigation On Firing Behavior of the Spark-Ignition Engine Fueled with Methanol, Liquefied Petroleum Gas (LPG), and Methanol/LPG During Cold Start, *Energy & Fuels, 22* (2008), 6, pp. 3779-3784

[4] Chen, Z., *et al*., Experimental Investigation On Performance and Combustion Characteristics of Spark-Ignition Dual-Fuel Engine Fueled with Methanol/Natural Gas, *Applied Thermal Engineering, 150* (2019), pp. 164-174

[5] Chen, Z., *et al*., Parametric Study On Effects of Excess Air/Fuel Ratio, Spark Timing, and Methanol Injection Timing On Combustion Characteristics and Performance of Natural Gas/Methanol Dual-Fuel Engine at Low Loads, *Energy Conversion and Management, 210* (2020), p. 112742

[6] Xu, C., *et al*., Experimental and Numerical Study On Laminar Premixed Flame Characteristics of 2-Ethylfuran, *Combustion and Flame, 234* (2021), p. 111631

[7] Chen, G., *et al*., The Content of Hydrogen to the Effect On the Combustion Characteristics of Biomass-Derived Syngas, *Thermal Science, 26* (2022), 6 part B, pp. 5267-5276

[8] Zhang, N., *et al*., On the Laminar Combustion Characteristics of Natural Gas-Syngas-Air Mixtures, *Thermal Science, 22* (2018), 5, pp. 2077-2086

[9] Wu, Y., *et al*., Understanding the Antagonistic Effect of Methanol as a Component in Surrogate Fuel Models: A Case Study of Methanol/N-Heptane Mixtures, *Combustion and Flame, 226* (2021), pp. 229-242

[10] Baloo, M., *et al.,* Effect of Iso-Octane/Methane Blend On Laminar Burning Velocity and Flame Instability, *Fuel, 144* (2015), pp. 264-273

[11] Sileghem, L., *et al*., Laminar Burning Velocities of Primary Reference Fuels and Simple Alcohols, *Fuel, 115* (2014), pp. 32-40

[12] Gulder, Ö. L., Laminar Burning Velocities of Methanol, Isooctane and Isooctane/Methanol Blends, *Combustion Science and Technology, 33* (1983), 1-4, pp. 179-192

[13] Wang, Q., *et al*., Laminar Combustion Characteristics of Methane/Methanol/Air Mixtures: Experimental and Kinetic Investigations, *Case Studies in Thermal Engineering, 41* (2023), p. 102593

[14] Faghih, M., Chen, Z., The Constant-Volume Propagating Spherical Flame Method for Laminar Flame Speed Measurement, *Science Bulletin, 61* (2016), 16, pp. 1296-1310

[15] Xu, C., *et al*., Effect of Hydrogen Addition On the Laminar Burning Velocity of N-Decane/Air Mixtures: Experimental and Numerical Study, *International Journal of Hydrogen Energy* (2022)

[16] Konnov, A. A., *et al*., A Comprehensive Review of Measurements and Data Analysis of Laminar Burning Velocities for Various Fuel+Air Mixtures, *Progress in Energy and Combustion Science, 68* (2018), pp. 197-267

[17] Kelley, A. P., Law, C. K., Nonlinear Effects in the Extraction of Laminar Flame Speeds From Expanding Spherical Flames, *Combustion and Flame, 156* (2009), 9, pp. 1844-1851

[18] Xu, C., *et al*., Laminar Burning Velocity of 2-Methylfuran-Air Mixtures at Elevated Pressures and Temperatures: Experimental and Modeling Studies, *Fuel, 231* (2018), pp. 215-223

[19] Li, J., *et al*., A Comprehensive Kinetic Mechanism for CO, CH2O, and CH3OH Combustion, *International Journal of Chemical Kinetics, 39* (2007), 3, pp. 109-136

[20] ***, San Diego Mechanism, "Chemical-Kinetic Mechanisms for Combustion Applications", San Diego Mechanism web page, Mechanical and Aerospace Engineering (Combustion Research), University of California at San Diego, http://combustion.ucsd.edu

[21] Zhang, X., *et al*., Investigation On the Oxidation Chemistry of Methanol in Laminar Premixed Flames, *Combustion and Flame, 180* (2017), pp. 20-31

[22] Metcalfe, W. K., *et al*., A Hierarchical and Comparative Kinetic Modeling Study of C1 − C2 Hydrocarbon and Oxygenated Fuels, *International Journal of Chemical Kinetics, 45* (2013), 10, pp. 638-675

[23] Mitu, M., Brandes, E., Explosion Parameters of Methanol–Air Mixtures, *Fuel, 158* (2015), pp. 217-223

[24] Zhang, Z., *et al*., Measurements of Laminar Burning Velocities and Markstein Lengths for Methanol–Air–Nitrogen Mixtures at Elevated Pressures and Temperatures, *Combustion and Flame, 155* (2008), 3, pp. 358-368

[25] Saeed, K., Stone, C. R., Measurements of the Laminar Burning Velocity for Mixtures of Methanol and Air From a Constant-Volume Vessel Using a Multizone Model, *Combustion and Flame, 139* (2004), 1-2, pp. 152-166

[26] Metghalchi, M., Keck, J. C., Burning Velocities of Mixtures of Air with Methanol, Isooctane, and Indolene at High Pressure and Temperature, *Combustion and Flame, 48* (1982), pp. 191-210

[27] Omari, A., Tartakovsky, L., Measurement of the Laminar Burning Velocity Using the Confined and Unconfined Spherical Flame Methods – a Comparative Analysis, *Combustion and Flame, 168* (2016), pp. 127-137

[28] Chen, Z., *et al.*, High Temperature Ignition and Combustion Enhancement by Dimethyl Ether Addition to Methane–Air Mixtures, *Proceedings of the Combustion Institute, 31* (2007), 1, pp. 1215-1222

[29] Law, C. K., Sung, C. J., Structure, Aerodynamics, and Geometry of Premixed Flamelets, *Progress in Energy and Combustion Science, 26* (2000), 4, pp. 459-505

[30] Wu, F., *et al.*, Measurement and Correlation of Laminar Flame Speeds of CO and C2 Hydrocarbons with Hydrogen Addition at Atmospheric and Elevated Pressures, *International Journal of Hydrogen Energy, 36* (2011), 20, pp. 13171-13180

[31] Lapalme, D., *et al.,* Assessment of the Method for Calculating the Lewis Number of H2 /CO/CH4 Mixtures and Comparison with Experimental Results, *International Journal of Hydrogen Energy, 42* (2017), 12, pp. 8314-8328

[32] Bechtold, J. K., Matalon, M., The Dependence of the Markstein Length On Stoichiometry, *Combustion and Flame, 127* (2001), 1-2, pp. 1906-1913

[33] Tang, C. L., *et al.*, Determination, Correlation, and Mechanistic Interpretation of Effects of Hydrogen Addition On Laminar Flame Speeds of Hydrocarbon–Air Mixtures, *Proceedings of the Combustion Institute, 33* (2011), 1, pp. 921-928

[34] Cheng, Y., *et al.*, Kinetic Analysis of H 2 Addition Effect On the Laminar Flame Parameters of the C1–C4 N-Alkane-Air Mixtures: From One Step Overall Assumption to Detailed Reaction Mechanism, *International Journal of Hydrogen Energy, 40* (2015), 1, pp. 703-718

[35] Chen, Z., On the Extraction of Laminar Flame Speed and Markstein Length From Outwardly Propagating Spherical Flames, *Combustion and Flame, 158* (2011), 2, pp. 291-300

[36] Clavin, P., Williams, F. A., Effects of Molecular Diffusion and of Thermal Expansion On the Structure and Dynamics of Premixed Flames in Turbulent Flows of Large Scale and Low Intensity, *Journal of Fluid Mechanics, 116* (1982), pp. 251-282

Received: 01.02.2023.
Revised: 13.04.2023.
Accepted: 13.07.2023.